Structural characterization of a monomeric chemokine: Monocyte chemoattractant protein-3

Key-Sun Kim[1,a], Krishnakumar Rajarathnam[a], Ian Clark-Lewis[b], Brian D. Sykes[a,*]

[a]*The Protein Engineering Network of Centres of Excellence (PENCE) and Department of Biochemistry, University of Alberta, Edmonton, Alberta T6G 2S2, Canada*

[b]*The Biomedical Research Centre and Department of Biochemistry and Molecular Biology, University of British Columbia, Vancouver, British Columbia V6T 1Z3, Canada*

Received 9 July 1996; revised version received 23 August 1996

Abstract **^{1}H-NMR spectroscopy and analytical ultracentrifugation studies reveal that monocyte chemoattractant protein-3 (MCP-3) is a monomer. NMR solution structure shows that MCP-3 adopts an α/β fold similar to what is observed in structures of other known chemokines. However, MCP-3 is unique in that it does not show a propensity to form dimers. The closely related chemokines MCP-1 and MCP-2 show a monomer-dimer equilibrium in sedimentation equilibrium studies (~0.2–2 mg/ml). As these proteins are present at nanomolar concentrations in vivo, the results suggest that they are monomeric at functional concentrations and that the monomer is the functionally significant form of MCP-1, MCP-2 and MCP-3.**

Key words: Monocyte chemotactic protein; NMR; Solution structure; Monomer-dimer

1. Introduction

Monocyte chemoattractant protein (MCP)-1 [1], MCP-2 and MCP-3 [2,3] are members of the family of chemoattractant cytokines (chemokines). Chemokines stimulate the migration and accumulation of various types of white blood cells and are divided into two subfamilies according to the position of the first two cysteine residues [4,5]. For the CXC chemokines, e.g. interleukin 8 (IL-8), the first two cysteines are separated by one residue, whereas for the CC chemokines, including MCP-1, MCP-2, MCP-3, RANTES and MIP-1β, the first two cysteines are adjacent. The structures of a number of chemokines have been solved by NMR and X-ray crystallography methods and all show a similar structural topology consisting of 3 anti-parallel β strands and an overlying COOH-terminal α helix [6]. Whilst CXC chemokines, such as IL-8 and MGSA, dimerize by formation of a central six stranded β sheet [7–10], the CC chemokines, such as MIP-1β and RANTES, dimerize in an end on end configuration through interactions that involve the NH_2-terminal regions of the two subunits [11–13]. In addition, PF-4 and NAP-2, which are CXC chemokines, form tetramers and show both IL-8 and RANTES type interfaces [14,15].

In addition, the two subfamilies are functionally distinct. The CXC chemokines are predominantly neutrophil chemoattractants, whereas the CC chemokines attract other cell types, but not neutrophils. MCP-1, MCP-2 and MCP-3 share considerable sequence similarity (60–71%) (Fig. 1). Despite this, functional differences between them are apparent. MCP-3 stimulates eosinophils in addition to other cell types, whereas MCP-1 does not affect eosinophils [4]. MCP-2 appears to have similar activities to MCP-3, but is less potent than MCP-3 [16]. In addition other differences including intracellular signaling mechanisms have been reported [17].

The multiple functional activities of MCP-3 suggest that comparison of its structure with other chemokines, as well as its structure-activity relationships, will be of importance for understanding its mechanism of action in inflammation. Here we compare the quaternary structure of the three MCP proteins: MCP-1, MCP-2 and MCP-3; and furthermore describe the ^{1}H-NMR solution structure of MCP-3 which reveals that it is a monomer. The results are discussed in terms of their implications for the structure and functions of the chemokine family.

2. Materials and methods

All proteins were synthesized, purified and characterized as described previously [18]. The synthesis was accomplished by automated solid-phase synthesis (Applied Biosystems Model 430A) using the *t*-butyloxycarbonyl and benzyl protection strategy, deprotection with hydrogen fluoride, and then folding by air oxidation and purification by reverse-phase HPLC. Purity and the correctness of the product were assessed by reverse-phase HPLC and mass spectrometry. The samples for NMR were prepared by dissolving the lyophilized protein in either 90% H_2O/10% D_2O or 99.9% D_2O and the pH was adjusted to 5.10 ± 0.05 (glass electrode, uncorrected) with concentrated NaOD.

Sedimentation equilibrium studies were carried out on a Beckman Spinco Model E analytical ultracentrifuge using Raleigh interference optics. The average molecular weights (M_{av}) from sedimentation equilibrium runs were calculated using the following equation:

$$M_{av} = \frac{2RT}{(1-\upsilon\rho)} \frac{d(\ln C)}{\omega^2 d(r^2)} \quad (1)$$

where R is the universal gas constant and is equal to 8.314×10^7 erg/mol per K, T is the temperature in K, ρ is the solvent density which was calculated to be 1.005, ω is the angular velocity (rpm × 2π/60) in rad/s, υ is the partial specific volume of the protein (calculated from the amino acid composition), and C is concentration in units of mg/ml.

All ^{1}H-NMR experiments were performed on a Varian Unity 600 NMR spectrometer. Standard pulse sequences were employed for res-

*Corresponding author. Fax: (1) (403) 492-1473.

[1] *Present address:* Structural Biology Center, Korea Institute of Science and Technology, Seoul 130-650, South Korea.

Abbreviations: IL-8, interleukin-8; MCP, monocyte chemoattractant protein; MGSA, melanoma growth stimulatory activity; MIP-1β, macrophage inhibitory protein-1β; NAP-2, neutrophil activating peptide-2; PF-4, platelet factor-4; DQF-COSY, double quantum filtered correlation spectroscopy; NOE, nuclear Overhauser effect; NOESY, NOE spectroscopy; RANTES, regulated on activation normal T cell expressed; HPLC, high-performance liquid chromatography; RMS, root-mean-square

PII S0014-5793(96)01024-1

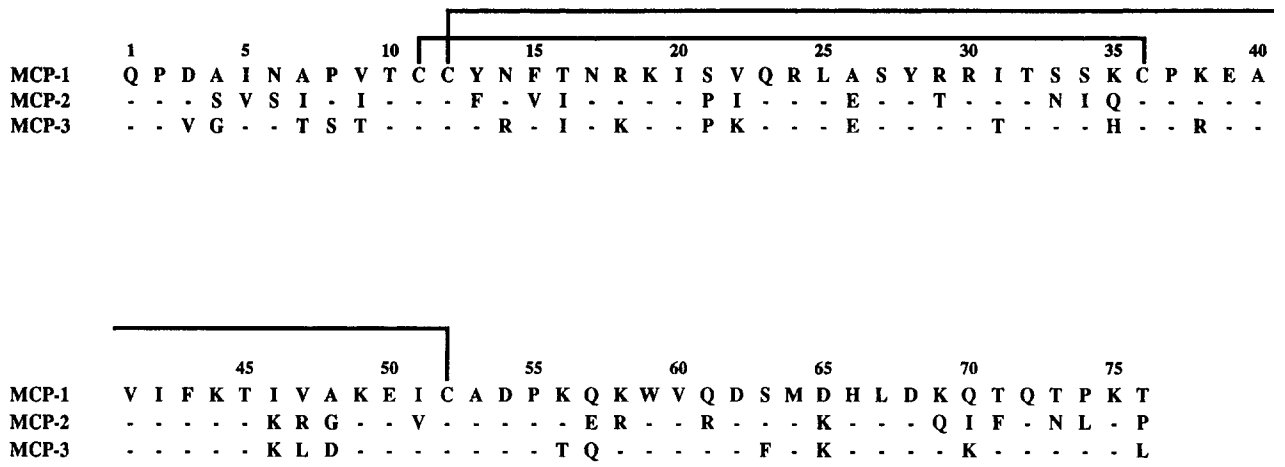

Fig. 1. Alignment of the primary amino acid sequence of MCP-1, MCP-2 and MCP-3. Disulfide bonds between conserved cysteines are indicated.

onance assignments: PECOSY [19], DQF-COSY [20], TOCSY [21] and NOESY [22]. TOCSY spectra were acquired with mixing times of 45 and 55 ms and NOESY spectra with mixing times of 70 and 150 ms. All spectra were recorded in phase sensitive mode [23] and were referenced to externally added DSS.

^{1}H-NMR relaxation rates ($R_2=1/T_2$) were measured using the Carr-Purcell-Merboom-Gill spin-echo pulse sequence [24]. The ^{1}H-NMR relaxation time T_2 for methyl protons is dependent on the rotation correlation time τ_c by the equation

$$\frac{1}{T_2} = (m-1)\left(\frac{3}{20}\frac{\gamma^4\hbar^2}{r^6}\right)\left[\frac{1-3\cos^2\theta}{2}\right]^2\left\{3\tau_c + \frac{5\tau_c}{1+\omega_o^2\tau_c^2} + \frac{2\tau_c}{1+4\omega_o^2\tau_c^2}\right\} \quad (2)$$

where $\hbar$ is Plank's constant, γ is the gyromagnetic ratio, r is the distance between two methyl protons, τ_c is the overall rotational correlation time, m is the number of protons, θ is 90° for a CH_3 group, ω_o is the spectrometer frequency, and internal rotation of the CH_3 group is assumed to be rapid [25]. Upon substitution for the known constants and assuming $(\omega_o\tau_c)^2 \gg 1$ in Eq. 2 gives

$$R_2 = 1/T_2 = \lambda\tau_c \quad (3)$$

where $\lambda=3.75\times10^9$ s^{-2}. The Stokes-Einstein equation indicates that τ_c and hence R_2 is proportional to the molecular weight for spherical proteins. Typically, for a molecular weight (MW) of 10000, τ_c is $\sim5\times10^{-9}$ s at 25°C in H_2O [26].

NOE intensities for structure calculations were measured from the 150 ms NOESY spectrum by volume integration, and were converted into distances. The distance restraints were divided into 3 groups with ranges of 1.8–2.7, 1.8–3.5, and 2.3–5.0 Å and pseudoatoms are corrected appropriately. Structures were calculated using the hybrid distance geometry-dynamical simulated annealing program X-PLOR [27]. A total of 214 long-range ($|i-j|\geq5$) NOEs, 66 medium-range ($2\leq|i-j|\leq4$) NOEs, 178 sequential NOEs, and 474 intra-residue NOEs were used for structure calculations. In addition, 58 ϕ restraints, 25 ψ restraints, 5 $\chi1$ restraints and 16 backbone hydrogen bond restraints were added at the later stage of structure calculations.

3. Results

Sedimentation equilibrium ultracentrifugation studies of MCP-1, MCP-2, and MCP-3 were carried out to assess whether they are monomers or form higher order quaternary structures under the conditions studied. The sedimentation profiles are shown in Fig. 2. The slopes of these plots are proportional to the molecular weights (Eq. 1). For MCP-3 the profile is linear, indicative of the absence of higher order species. The observed MW of 8930 calculated from the slope is very close to the actual MW of 8957, indicating that MCP-3 is a monomer. For MCP-1 (MW 8685) and MCP-2 (MW 8915), the sedimentation profile is not linear. This is indicative of the presence of higher order species and the calculated MW values (~11000 and ~13700 for MCP-1 and MCP-2, respectively) indicate a distribution between monomers and dimers in the concentration range of these experiments (~0.2–2.0 mg/ml).

The amino acid Val^{60} is conserved among MCP-1, MCP-2, and MCP-3 and is expected to be in the similar environment given the high sequence homology (Fig. 1). NMR relaxation rates (R_2) for the protons of the upfield CγH$_3$ groups of Val^{60} of these proteins were measured in order to calculate the rotational correlation time (τ_c) (Fig. 3). The calculated T_2 values for MCP-1 and MCP-2 (0.023, 0.021 s, respectively) are shorter than those for MCP-3 (0.038 s) indicating that MCP-1 and MCP-2 have relatively higher molecular weights

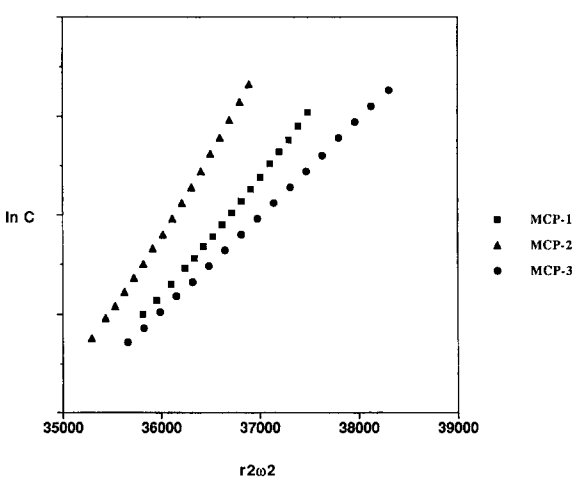

Fig. 2. Average molecular weight determination by sedimentation equilibrium of MCP-1, MCP-2 and MCP-3. Plots of ln C vs. $r^2\omega^2$ are shown, where C is the concentration and r is the distance from the axis of rotation and ω is the angular velocity. Sedimentation equilibrium runs of all the proteins were carried out at a concentration of ~1 mg/ml in 100 sodium phosphate, pH 6.6. Runs carried out at rotor speeds between 24000 and 32000 rpm depending on the sample for a period of 48 h. Molecular weights were calculated from the slopes of the plot using Eq. 1.

Table 1
Proton resonace assignments of MCP-3 at 30°C, pH 5.1[a,b]

Residue	NH	$C^{\alpha}H$	$C^{\beta}H$	Others
Gln^{1}		4.69	2.62, 2.09	$C^{\gamma}H$ 2.44
Pro^{2}		4.52	2.22, 1.89	$C^{\gamma}H$ 2.01; $C^{\delta}H$ 3.58, 3.70
Val^{3}	8.30	4.14	2.07	$C^{\gamma}H_3$ 0.97, 1.00
Gly^{4}	8.47	3.98		
Ile^{5}	7.97	4.21	1.85	$C^{\gamma}H$ 1.41, 1.16; $C^{\gamma}H_3$ 0.89; $C^{\delta}H_3$ 0.83
Asn^{6}	8.52	4.81	2.91, 2.80	
Thr^{7}	8.18	4.35	4.28	$C^{\gamma}H_3$ 1.20
Ser^{8}	8.35	4.55	3.93, 3.88	
Thr^{9}	8.38	4.38	4.19	$C^{\gamma}H_3$ 1.15
Thr^{10}	8.24	4.34	4.14	$C^{\gamma}H_3$ 1.22
Cys^{11}	8.12	4.99	2.80, 2.54	
Cys^{12}	8.36	4.64	2.41, 2.72	
Tyr^{13}	[c]	4.42	3.13, 2.72	$C^{\delta}H$ 7.11; $C^{\epsilon}H$ 6.77
Arg^{14}	7.45	4.32	1.78, 1.66	$C^{\gamma}H$ 1.50; $C^{\delta}H$ 3.20; $N^{\epsilon}H$ 7.18
Phe^{15}	8.54	4.81	2.91, 3.23	$C^{\delta}H$ 7.01; $C^{\epsilon}H$ 7.20; $C^{\zeta}H$ 7.11
Ile^{16}	8.72	4.41	2.18	$C^{\gamma}H$ 1.62, 1.73; $C^{\gamma}H_3$ 1.25; $C^{\delta}H_3$ 1.05
Asn^{17}	8.64	5.06	2.95	$N^{\delta}H_2$ 7.64, 6.95
Lys^{18}	7.39	4.29	1.71, 1.59	$C^{\gamma}H$ 1.29
Lys^{19}	7.71	2.52	1.16, 1.09	$C^{\gamma}H$ 0.70, 0.90; $C^{\delta}H$ 1.35
Ile^{20}	6.14	4.32	1.64	$C^{\gamma}H$ 1.47, 1.05; $C^{\gamma}H_3$ 0.84; $C^{\delta}H_3$ 0.83
Pro^{21}		4.37	2.35, 1.75	$C^{\gamma}H$ 1.98 1.93; $C^{\delta}H$ 3.37, 3.78
Lys^{22}	8.26	3.27	1.31, 1.13	$C^{\gamma}H$ 0.63; $C^{\delta}H$ 0.85;$C^{\epsilon}H$ 1.03
Gln^{23}	8.71	4.18	2.06	$C^{\gamma}H$ 2.43, 2.37; $N^{\epsilon}H_2$ 7.55, 6.89
Arg^{24}	7.75	4.32	2.07, 1.78	$C^{\gamma}H$ 1.66;$C^{\delta}H$ 3.13, 3.22; $N^{\epsilon}H$ 7.40
Leu^{25}	7.50	4.34	1.92, 1.28	$C^{\gamma}H$ 1.56; $C^{\delta}H_3$ 0.28, 0.52
Glu^{26}	9.15	4.65	1.93, 1.73	$C^{\gamma}H$ 2.21
Ser^{27}	8.08	4.81	4.02, 4.08	
Tyr^{28}	8.62	5.74	2.42, 2.90	$C^{\delta}H$ 6.77, $C^{\epsilon}H$ 6.86
Arg^{29}	8.59	4.59	1.84, 1.70	$C^{\gamma}H$ 1.35; $C^{\delta}H$ 3.05, 3.17; $N^{\epsilon}H$ 7.54; $N^{\eta}H$ 6.88
Arg^{30}	8.86	5.18	1.73, 2.09	$C^{\gamma}H$ 1.80, 1.65; $C^{\delta}H$ 3.27; $N^{\epsilon}H$ 7.44
Thr^{31}	8.41	4.58	4.59	$C^{\gamma}H_3$ 1.24
Thr^{32}	8.32	4.51	4.32	$C^{\gamma}H_3$ 1.21
Ser^{33}	8.43	4.51	4.02, 3.91	
Ser^{34}	8.52	4.34	3.86	
His^{35}	8.13	4.69	3.11, 3.35	
Cys^{36}	7.68	5.17	2.68, 3.36	
Pro^{37}		4.38	2.42, 2.00	$C^{\gamma}H$ 2.18, 2.08; $C^{\delta}H$ 3.90, 3.67
Arg^{38}	7.18	4.55	1.71, 1.90	$C^{\gamma}H$ 1.53; $C^{\delta}H$ 3.06; $N^{\epsilon}H$ 7.15
Glu^{39}	8.63	4.08	1.94	$C^{\gamma}H$ 2.31, 2.18
Ala^{40}	8.12	4.97	1.57	
Val^{41}	8.42	4.46	1.36	$C^{\gamma}H_3$ 0.60, 0.12
Ile^{42}	8.99	4.94	1.62	$C^{\gamma}H$ 1.41, 0.90; $C^{\gamma}H_3$ 0.74; $C^{\delta}H_3$ 0.65
Phe^{43}	9.30	5.31	2.93, 3.13	$C^{\delta}H$ 7.24; $C^{\epsilon}H$ 6.91; $C^{\zeta}H$ 7.26
Lys^{44}	9.01	5.38	2.00, 1.85	$C^{\gamma}H$ 1.40; $C^{\delta}H$ 1.64; $C^{\epsilon}H$ 2.95
Thr^{45}	9.10	5.22	4.78	$C^{\gamma}H_3$ 1.22
Lys^{46}	8.66	4.22	1.76, 2.03	$C^{\gamma}H$ 1.40
Leu^{47}	7.69	4.50	1.81, 1.56	$C^{\gamma}H$ 1.59; $C^{\delta}H_3$ 0.93, 0.87
Asp^{48}	8.07	4.31	3.03, 2.68	
Lys^{49}	7.34	4.58	1.75, 1.84	$C^{\gamma}H$ 1.31, $C^{\delta}H$ 1.44, $C^{\epsilon}H$ 3.01
Glu^{50}	8.49	5.47	2.43, 1.95	$C^{\gamma}H$ 2.00, 1.80
Ile^{51}	9.17	4.54	1.95	$C^{\gamma}H$ 1.23, 1.54; $C^{\gamma}H_3$ 1.12; $C^{\delta}H_3$ 0.88
Cys^{52}	8.86	5.07	3.48, 2.78	
Ala^{53}	9.85	4.99	1.32	
Asp^{54}	8.41	4.08	2.60, 1.64	
Pro^{55}		3.99	1.94	$C^{\gamma}H$ 1.72, 1.83; $C^{\delta}H$ 4.01, 3.93
Thr^{56}	8.26	4.04	4.20	$C^{\gamma}H_3$ 1.18
Gln^{57}	7.44	4.21	1.65, 1.85	$C^{\gamma}H$ 2.37, 2.23
Lys^{58}	8.77	3.77	1.94	$C^{\gamma}H$ 1.48; $C^{\delta}H$ 1.75, 1.65; $C^{\epsilon}H$ 3.05
Trp^{59}	8.26	4.28	3.05, 2.98	$C^{\delta 1}H$ 7.58; $N^{\epsilon 1}H$ 10.06; $C^{\epsilon 3}H$ 6.35; $C^{\zeta 2}H$ 7.38; $C^{\zeta 3}H$ 6.50; $C^{\eta 2}H$ 6.94
Val^{60}	5.71	2.79	1.78	$C^{\gamma}H_3$ −0.67, 0.42
Gln^{61}	7.20	3.97	2.14, 2.08	$C^{\gamma}H$ 2.40, 2.28; $N^{\epsilon}H_2$ 6.62, 7.40
Asp^{62}	8.64	4.44	2.89, 2.76	
Phe^{63}	8.60	4.56	3.54, 2.91	$C^{\delta}H$ 7.01; $C^{\epsilon}H$ 7.44; $C^{\zeta}H$ 7.38
Met^{64}	8.42	3.68	2.28, 2.11	$C^{\gamma}H$ 1.77 0.61; $C^{\epsilon}H_3$ 1.81
Lys^{65}	7.64	4.14	1.98, 1.77	$C^{\gamma}H$ 1.52; $C^{\delta}H$ 1.69; $C^{\epsilon}H_2$ 3.02
His^{66}	7.89	4.40	3.43, 3.24	$C^{\delta 2}H$ 6.70; $C^{\epsilon 1}H$ 7.22
Leu^{67}	8.16	4.09	2.24, 1.76	$C^{\gamma}H$ 2.01; $C^{\delta}H_3$ 1.11, 0.85
Asp^{68}	8.63	4.60	2.90, 2.77	
Lys^{69}	7.60	4.21	1.86, 1.91	$C^{\gamma}H$ 1.48; $C^{\delta}H$ 1.58; $C^{\epsilon}H$ 3.02

Table 1 (*continued*)

Residue	NH	$C^{\alpha}H$	$C^{\beta}H$	Others
Lys^{70}	7.89	4.28	1.91, 1.82	$C^{\gamma}H$ 1.48; $C^{\delta}H$ 1.70; $C^{\epsilon}H$ 3.04
Thr^{71}	7.97	4.35	4.28	$C^{\gamma}H_3$ 1.26
Gln^{72}	8.21	4.43	2.03, 2.14	$C^{\gamma}H$ 2.41
Thr^{73}	8.20	4.59	4.17	$C^{\gamma}H_3$ 1.27
Pro^{74}		4.43	2.31, 1.91	$C^{\gamma}H$ 2.04; $C^{\delta}H$ 3.86, 3.73
Lys^{75}	8.34	4.32	1.85, 1.75	$C^{\gamma}H$ 1.46; $C^{\delta}H$ 1.70; $C^{\epsilon}H$ 3.02
Leu^{76}	7.87	4.21	1.59	$C^{\gamma}H$ 1.59; $C^{\delta}H_3$ 0.86, 0.90

[a]Uncertainities in chemical shift are ±0.02 ppm.
[b]Gln-1 exists as a pyroglutamate.
[c]Not seen.

compared to MCP-3. The rotational correlation times were calculated (Eq. 3) to be ~13 ns for MCP-1 and MCP-2 and ~7 ns for MCP-3. Although absolute molecular weight cannot be calculated accurately from T_2 values, the τ_c values are appropriate for molecular weights of a dimer (~18 000) and a monomer (~9000), respectively [26]. The NMR solution structure of MCP-1 has been solved recently [28] and was shown to be a dimer which is consistent with the above results.

The NMR chemical shift assignments for MCP-3 was achieved using standard two-dimensional NMR techniques (Table 1). Scalar connectivities were established from TOCSY and DQF-COSY spectra and through-space connectivities were identified from the NOESY spectra. The secondary structure of MCP-3, on the basis of the characteristic sequential, medium- and long-range NOEs involving CαH and amide protons is shown in Fig. 4. The pattern of NOE-derived intra-chain distances was similar to that of other chemokines indicating that it has a similar folded structure. However, no inter-chain NOEs were found, suggesting that MCP-3 is a monomer, consistent with the R_2 and the sedimentation equilibrium studies. An examination of the chemical shifts of the residues at the N-terminus showed that the shifts are close to that expected for a random coil indicating that these residues are not involved in dimer formation [29]. The corresponding residues in MIP-1β and RANTES show chemical shifts which are characteristic of a β sheet [11,12].

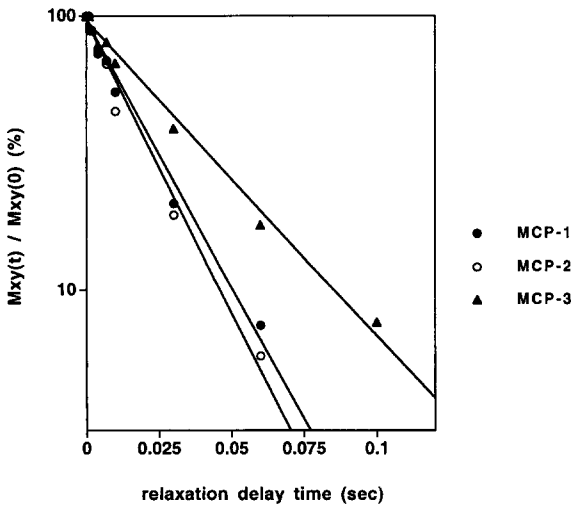

Fig. 3. Plot of the ^{1}HNMR transverse relaxation of the CH_3 resonances of Val^{60} in MCP-1, MCP-2 and MCP-3 as a function of different delay times.

30 structures were calculated using the program X-PLOR, all of which displayed good covalent geometry and showed minimal or no NOE violations. In these structures, there were no NOE violations greater than 0.5 Å and dihedral violations greater than 5°. The chemokine polypeptide fold consists of a relatively undefined N-terminal region and 3-antiparallel β-strands and a COOH-terminal α-helix crossing over the β-sheet (Fig. 5). The first 9 residues at the N-terminus and residues 70–76 in the C-terminus are undefined, and the observation that the shifts of these spin systems resemble those of a random coil support the observation that these terminal residues are unstructured [29]. The rmsd of the backbone atoms and heavy atoms for residues 11–68 are 0.75 and 1.4 Å, respectively. Residues 11–22 are relatively less well defined when compared to other chemokines which show a good definition for these residues. The rest of the structure (residues 23–68) is well defined with an rmsd of 0.5 Å for the backbone atoms and an rmsd of 1.1 Å for the heavy atoms.

It was observed that the tertiary fold of MCP-3 is very similar to that of other CXC and CC chemokines. Fig. 6 shows an alignment of the backbone atoms of the most ordered regions of MCP-3 with that of monomeric IL-8, a CXC chemokine and MIP-1β, a CC chemokine.

4. Discussion

Four lines of evidence indicate that MCP-3 does not have a propensity to dimerize and remains a monomer under a wide range of conditions. First, sedimentation equilibrium studies showed that MCP-3 exists as a monomer up to 2 mg/ml. Second, calculation of the rotational correlation time from NMR indicates that MCP-3 remains a monomer up to concentrations of ~20 mg/ml. Third, the chemical shifts of the residues in the N-terminal region indicate that these residues

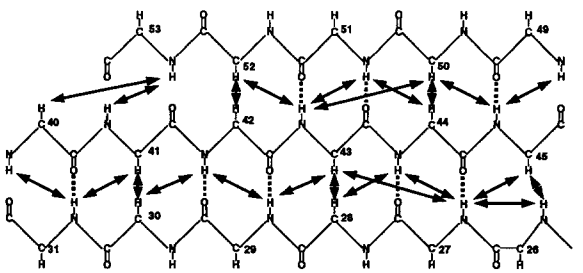

Fig. 4. Schematic representation of the anti-parallel β-sheet as determined from the NOE connectivities. Observed intrastrand NOEs are indicated by arrows and putative hydrogen bonds predicted from the NOE data are denoted by broken lines.

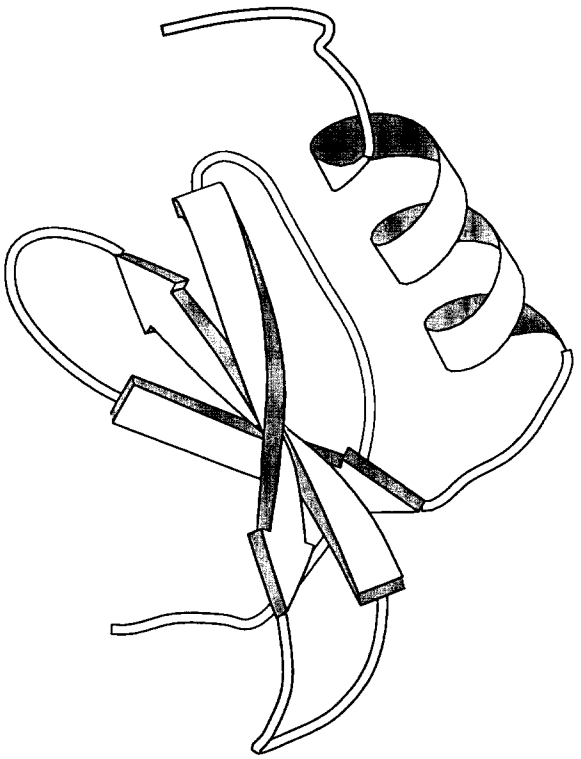

Fig. 5. Schematic showing the minimized average NMR structure of MCP-3. The figure was created using the program MOLSCRIPT [33].

are unstructured. Fourth, detailed analysis of the NOEs revealed no NOEs which can be attributed to inter-chain interactions. This is significant because the tertiary structures of all known chemokines to date, including three CC chemokines, are dimers or tetramers.

Sedimentation studies showed that both MCP-1 and MCP-2 are in a monomer-dimer equilibrium in the 0.2–2 mg/ml concentration range. As the functional concentration is at least 3 log units lower, these proteins are monomeric at the functional concentrations which is consistent with a previous sedimentation study of MCP-1 [30]. The MCP-2 used in these experiments has been shown to have the same spectrum of functional activities as MCP-3. This suggests that the difference in aggregation propensity of MCP-3 and MCP-2 is not responsible for the functional differences. Although MCP-2 is less potent than MCP-3, it seems unlikely that this is due to dimerization, because MCP-2 exists mostly as a monomer at functional concentrations. It is likely that multiple structural features contribute towards dimer formation, residues preceding the first cysteine at the N-terminus being most critical. Whereas the NMR solution structure indicated that MCP-1 was a dimer [28], a MCP-1 analog (9–76), missing the first first 8 residues was found to be predominantly a monomer by sedimentation and NMR studies (data not shown).

The folded structure of MCP-3 (Fig. 5) is similar to that of other chemokines representing both the CC and CXC subfamily. As expected from the greater sequence similarity and the common CC motif, the alignment of the backbone atoms was better with the CC chemokines. Thus, it has the characteristic chemokine fold: a disordered NH_2 terminal region, the CC motif, an extended loop, 3 β strands, and a COOH-terminal α helix. The major difference in the structure between MCP-3 and known structures of other CC chemokines, MCP-1, RANTES and MIP-1β, was in the NH_2-terminal region. The entire NH_2-terminal region in MCP-3 was disordered and suggests an intrinsic flexibility whereas the corresponding region is structured in MCP-1, RANTES and MIP-1β. This region of the protein has been shown to play a role in CXC chemokines for differential binding to the two receptors in neutrophils [6]. Future studies involving mutagenesis and synthesis of chimeric proteins should reveal the relevance of this structural flexibility for function.

MCP-3 is the first chemokine reported which remains monomeric to concentrations used in structural determinations (~20 mg/ml). I-309, a CC chemokine, has shown to be a monomer at sedimentation concentrations [30] and the K_d of IL-8 [30,31] and MCP-1 [30] has been shown to be in the μM range. The in vitro functional response of a monomeric IL-8 which cannot dimerize was shown to be indistinguishable from that of the native protein [32].

The results suggest that MCP-1, MCP-2 and MCP-3 normally function as monomers and that dimerization is not essential for receptor binding and activation in vitro. It remains to be determined whether dimerization is critical in vivo for factors that has not yet been examined. It is believed that it is the heparin bound chemokines which bind to the receptor and whether dimerization is essential for heparin binding remains to be investigated.

Fig. 6. Comparison of MCP-3 (thick black) with MIP-1β (thick gray) and monomeric IL-8 (thin black). The best-fit superpositions of the backbone atoms are shown.

Acknowledgements: We thank Dr. Cyril Kay for access to the ultracentrifuge; and Philip Owen, Luen Vo, Peter Borowski and Jennifer Anderson for chemical synthesis. We acknowledge the assistance of Gerry McQuaid for maintenance of NMR spectrometer; and Les Hicks for sedimentation equilibrium studies. This work was supported by the Protein Engineering Network of Centres of Excellence (PENCE), the Arthritis Society of Canada, and National Institutes of Health USA R01 GM50969-01 to I.C.-L.

References

[1] Yoshimura, T., Yukhi, N., Moore, S.K., Appella, E., Lerman, M.I. and Leonard, E.J. (1989) FEBS Lett. 244, 487–493.
[2] Van Damme, J., Proost, P., Lenaerts, J.-P. and Opdenakker, G. (1992) J. Exp. Med. 176, 59–65.
[3] Opdenakker, G., Froyen, G., Fiten, P., Proost, P. and Van Damme, J. (1993) Biochem. Biophys. Res. Commun. 191, 535–542.
[4] Baggiolini, M., Dewald, B. and Moser, B. (1994) Adv. Immunol. 55, 97–179.
[5] Miller, M.D. and Krangel, M.S. (1992) Crit. Rev. Immunol. 12, 17–46.
[6] Clark-Lewis, I., Kim, K.-S., Rajarathnam, K. Gong, J.-H., Dewald, B., Moser, B.M., Baggiolini, M. and Sykes, B.D. (1995) J. Leuk. Biol. 57, 703–711.
[7] Clore, G.M., Appella, E., Yamada, M., Matsushima, K. and Gronenborn, A.M. (1990) Biochemistry 29, 1689–1696.
[8] Baldwin, E.T., Weber, I.T., Charles, R.S., Xuan, J.-C., Appella, E., Yamada, M., Matsushima, K., Edwards, B.F.P., Clore, G.M., Gronenborn, A.M. and Wlodawer, A. (1991) Proc. Natl. Acad. Sci. USA 88, 502–506.
[9] Fairbrother, W.J., Reilly, D., Colby, T., Hesselgesser, J. and Horuk, R. (1994) J. Mol. Biol., 242, 252–270.
[10] Kim, K.-S., Clark-Lewis, I. and Sykes, B.D. (1994) J. Biol. Chem. 269, 32909–32915.
[11] Lodi, P.J., Garrett, D.S. Kuszewski, J., Tsang, M.L-S., Weatherbee, J.A., Leonard, W.J., Gronenborn, A.M. and Clore, G.M. (1994) Science 263, 1762–1767.
[12] Skelton, N.J., Aspiras, F., Ogez, J. and Schall, T.J. (1995) Biochemistry 34, 5329–5342.
[13] Chung, C.-W., Cooke, R.M., Proudfeet, A.E.I. and Wells, T.N.C. (1995) Biochemistry 34, 9307–9314.
[14] Malkowski, M.G., Wu, J.Y., Lazar, J.B., Johnson, P.H. and Edwards, B.F.P. (1995) J. Biol. Chem. 270, 7077–7087.
[15] Zhang, X., Chen, L., Bancroft, D.P., Lai, C.K. and Maione, T.E. (1994) Biochemistry 33, 8361–8366.
[16] Weber, M, Uguccioni, M., Ochensberger, B., Baggiolini, M., Clark-Lewis, I. and Dahinden, C.A. (1995) J. Immunol. 154, 4166–4172.
[17] Sozzani, S., Zhou, D., Locati, M., Rieppi, M., Proost, P., Magazin, M., Vita, N., Van Damme, J. and Mantovani, A. (1994) J. Immunol. 152, 3615–3622.
[18] Clark-Lewis, I., Moser, B., Walz, A. Baggiolini, M., Scott, G.J. and Aebersold, R. (1991) Biochemistry 30, 3128–3135.
[19] Mueller, L. (1987) J. Magn. Reson. 72, 191–196.
[20] Rance, M., Sørensen, O.W., Bodenhausen, G., Wagner, G., Ernst, R.R. and Wüthrich, K. (1983) Biochem. Biophys. Res. Commun. 117, 479–485.
[21] Davis, D.G. and Bax, A. (1985) J. Am. Chem. Soc. 107, 2821–2822.
[22] Jeener, J., Meier, B.H., Bachmann, P. and Ernst, R.R. (1979) J. Chem. Phys. 71, 4546–4553.
[23] States, D.J., Haberkorn, R.A. and Reuben, D.J. (1982) J. Magn. Reson. 48, 286–292.
[24] Meiboom, S. and Gill, D. (1958) Rev. Sci. Instrum. 29, 688–691.
[25] Hoyt, D.W., Harkins, R.N., Debanne, M.T., O'Connor-McCourt, M. and Sykes, B.D. (1994) Biochemistry 33, 15283–15292.
[26] Brauer, M. and Sykes, B.D. (1987) in: Phosphorus NMR in Biology (Burt, C.T. ed.) pp. 153–184, CRC Press, Boca Raton, FL.
[27] Brünger, A.T. (1992) X-PLOR. A System for X-ray Crystallography and NMR, Yale University Press, New Haven, CT.
[28] Handel, T.M. and Domaille, P.J. (1996) Biochemistry 35, 6569–6584.
[29] Wishart, D.S., Sykes, B.D. and Richards, F.M. (1991) J. Mol. Biol. 222, 311–333.
[30] Paolini, J.F., Willard, D., Consler, T., Luther, M. and Krangel, M.S (1994) J. Immunol. 153, 2704–2717.
[31] Burrows, S.D., Doyle, M.L., Murphy, K.P., Franklin, S.G., White, J.R., Brooks, I., McNulty, D.E., Scott, M.O., Knutson, J.R., Porter, D., Young, P.R. and Hensley, P. (1994) Biochemistry 33, 12741–12745.
[32] Rajarathnam, K., Sykes, B.D., Kay, C.M., Dewald, B., Geiser, T., Baggiolini, M. and Clark-Lewis, I. (1994) Science 264, 90–92.
[33] Kraulis, P. (1991) J. Appl. Crystallogr. 24, 946-950.